Journal of Applied Physics

Manipulating heat transport of photoluminescent composites in LEDs/LDs

Cite as: J. Appl. Phys. **130**, 070906 (2021); https://doi.org/10.1063/5.0056228
Submitted: 07 May 2021 . Accepted: 22 July 2021 . Published Online: 18 August 2021

Bin Xie, Run Hu, and Xiaobing Luo

Journal of Applied Physics PERSPECTIVE scitation.org/journal/jap

Manipulating heat transport of photoluminescent composites in LEDs/LDs

Cite as: J. Appl. Phys. **130**, 070906 (2021); doi: 10.1063/5.0056228
Submitted: 7 May 2021 · Accepted: 22 July 2021 ·
Published Online: 18 August 2021

View Online Export Citation CrossMark

Bin Xie,[1,2] Run Hu,[1,a)] and Xiaobing Luo[1,2]

AFFILIATIONS

[1]School of Energy and Power Engineering, Huazhong University of Science and Technology, Wuhan 430074, China
[2]Wuhan National Laboratory for Optoelectronics, Huazhong University of Science and Technology, Wuhan 430074, China

Note: This paper is part of the Special Topic on Engineering and Understanding of Thermal Conduction in Materials.
[a)]**Author to whom correspondence should be addressed:** hurun@hust.edu.cn

ABSTRACT

Photoluminescent composites play a critical role of light converters in light-emitting devices, especially in high-power light-emitting diodes and laser diodes, while the nonradiative Stokes loss in photoluminescent particles not only generates thermal phonons with temperature rise but also degrades their photonic/electronic properties. Moreover, these micro/nanoscale heat sources are usually dispersed in a low-thermal-conductivity polymer matrix, which makes it tough to dissipate heat out efficiently, resulting in significant thermal quenching. Reinforcing the heat dissipation of photoluminescent composites is considerably important and challenging since their optical performance will be easily damaged by the thermal reinforcement processes. In this Perspective, we briefly introduce the heat generation and transportation mechanisms in photoluminescent composites and then emphasize the recent progresses in heat manipulation of photoluminescent composites. Finally, we outline some challenges and possible solutions for addressing the thermal management of photoluminescent composites as well as some future directions in this field.

I. INTRODUCTION

After four generations of evolution, the lighting technology has made earth-shaking progress from candle lighting, incandescent lighting, and fluorescent lighting, to solid-state lighting (SSL).[1–3] The latest-generation SSL devices, mainly based on light-emitting diodes (LEDs), have attracted numerous attention in recent decades due to their high luminous efficiency, cost-effective fabrication, and low power consumption characteristics.[4–6] The most conventional white LEDs (WLEDs) are composed of blue LED chips and yellow–greenish phosphorescent composites (namely, the phosphor–polymer composites).[7,8] Although this configuration can meet most of the application requirements, there are still reasons for developing new packaging structures and phosphorescent materials. On the one hand, LED chips suffer from efficiency droop in high input current density, which inevitably limits the highest achievable luminous flux density of WLEDs.[9,10] On the other hand, the wide full-width-at-half-maximum (FWHM) of phosphor materials makes traditional WLEDs feature a low color rendering index (CRI) as well as limited color gamut.[11,12]

To remedy the defects of traditional WLEDs, the laser diode (LD) chip and quantum dots (QDs) were proposed as alternatives of LED chips and phosphor, respectively. Since the Auger recombination in LD no longer increases after the threshold driving current, the power-conversion efficiency of LD keeps increasing with power density, while the efficiency of LED decreases rapidly under increasing input power density.[13,14] Moreover, LD generates nearly monochromatic and collimating light with a narrow FWHM and a small divergent angle.[15,16] With these extraordinary characteristics, LD has been regarded as a strong competitor of LED in the high-power SSL applications.[17–21] The QDs, as luminescent nanocrystals, possess superior opto-electronic properties like high absorption coefficients, long carrier diffusion lengths, high quantum efficiencies, and size-tunable narrow emission spectra.[22–24] In the past few years, QDs not only have shown their great potential in the cost-effective yet high-performance photovoltaic applications, such as solar cells,[25,26] photodetectors,[27,28] and lasers,[29] but also have demonstrated commercial applications in LED lighting with high CRI and LED displays with wide color gamut.[30–34] It is predictable that in the very near future,

QD-WLEDs/WLDs will take the place of traditional WLEDs across a broad range of fields.

Although the future of QD-WLEDs/WLDs is bright, several challenges are certain to arise with the increase in input power density, particularly the thermal quenching (TQ) of luminescent particles under concentrated input optical power.[35,36] This is mainly attributed to the nonradiative recombination of excitons and extremely low thermal conductivity of polymer matrix, in which the luminescent particles are embedded.[37,38] As the nonradiative process generates heat inside the composites, the thermal phonons are restricted to the polymer matrix and unable to be dissipated out efficiently, resulting in the temperature rise therein. The high working temperature in turn decreases the quantum efficiency of luminescent particles and aggravates the temperature rise. Eventually, the quantum efficiency of luminescent particles decreases sharply, known as the thermal quenching (TQ) effect. With the increase in luminous flux density in WLEDs/WLDs, this problem will be more severe. More than that, QDs are more easily damaged by high temperature than crystallized phosphor because the thermally induced permanent trap states inside QDs are originated from the intrinsic difference in thermal expansion of the core, shell, and ligand materials.[39,40] Therefore, effective solutions are urgently needed to resolve the thermal challenge of luminescent particles before it becomes the bottleneck of high-power WLED/WLD applications.

In this Perspective, we first briefly introduce the heat generation and dissipation process in photoluminescent composites. Then, we mainly discuss recent progresses in heat transport manipulation theory and method of photoluminescent composites. Finally, we present a Perspective for future directions in this field.

II. BASIC THEORY

A. Heat generation and thermal quenching of luminescent particles

In a macroscopic view, the heat generated in luminescent particles, including phosphors and QDs, originates from the nonradiative recombination process of excitons. This heat energy causes temperature rise and eventually results in TQ of luminescent particles, while the underlying mechanisms of the TQ are quite complicated and divergent among different materials.[41–44]

For the Ce^{3+}- and Eu^{2+}-activated phosphors, there are mainly two theories for explaining the TQ mechanisms. The crossover theory that was proposed by Blasse and Grabmaier in the 1970s considers that the TQ is attributed to the nonradiative relaxation of excitons from the excited state to the ground state.[45] Figure 1(a) shows the configurational coordinate diagram in a phosphor. In this theory, TQ is originated from the nonradiative relaxation of an excited electron to the ground state once the temperature is high enough to overcome the activation energy E_a^{co}. From the theory, it is predictable that a more rigid phosphor host structure can reduce the probability of nonradiative relaxation and release the TQ. However, some phosphors with a rigid crystal structure still suffer from TQ such as $Ca_7Mg(SiO_4)_4:Eu^{2+}$, $CaMgSi_2O_6:Eu^{2+}$, and $Sr_6M_2Al_4O_{15}:Eu^{2+}$ (M = Y, Lu, Sc).[46,47] Therefore, Dorenbos proposed another theory—the thermal ionization theory—that TQ is because of the thermal ionization of the excited 5d electron of Ce^{3+}/Eu^{2+} to the conduction band of the host.[44] In this theory, the temperature should be high enough to overcome the activation energy E_a^i from the excited state to the conduction band minimum (CBM). Furthermore, Amachraa *et al.* unified the two dominant theories into a single predictive model for TQ by using *ab initio*

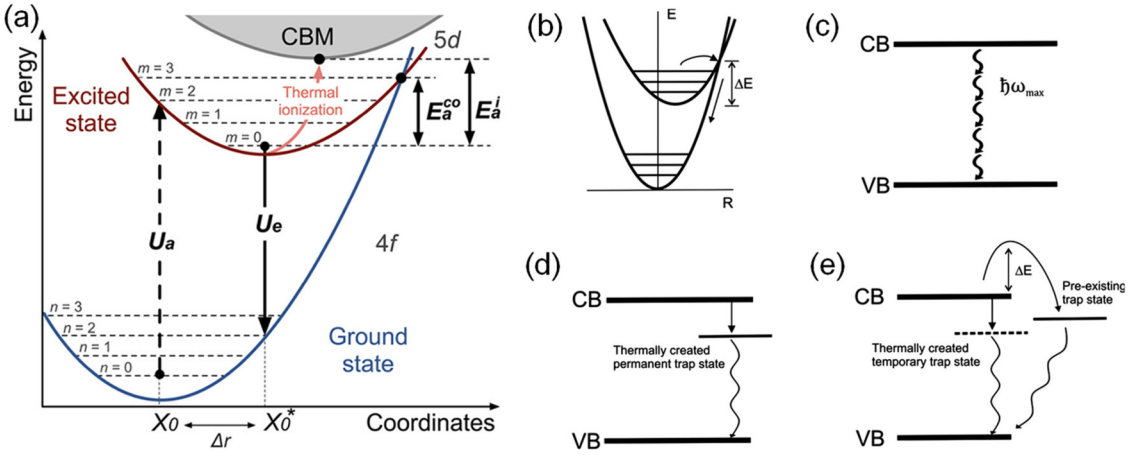

FIG. 1. (a) Configurational coordinate diagram for the activator in a phosphor. Excitation is originated from the vibrational level $n = 0$ of the ground state to the excited state, resulting in the absorption energy U_a. Relaxation is originated from the vibrational level $m = 0$ to the ground state, resulting in the emission energy. In the crossover model, TQ is caused by the nonradiative relaxation of an excited electron to the ground state. In the thermal ionization model, TQ is caused by the promotion of excited electrons to the conduction band minimum. Reproduced with permission from Amachraa *et al.*, Chem. Mater. **32**, 6256 (2020). Copyright 2020 American Chemical Society. Schematic diagram of luminescence quenching mechanisms in QDs: (b) intrinsic quenching based on thermally activated crossover, (c) intrinsic quenching based on multiphonon relaxation theory, (d) irreversible quenching related to traps, and (e) reversible quenching related to traps. Reprinted with permission from Zhao *et al.*, ACS Nano **6**, 9058 (2012). Copyright 2012 American Chemical Society.

molecular dynamics (AIMD) simulation.[48] They constructed the unified TQ model based on the measured TQ values of 29 oxide phosphors. According to this model, the local activator environment distribution with temperature in AIMD simulations is the indicator for TQ under the crossover mechanism. The host bandgap, the centroid shift, and the approximated crystal-field splitting are indicators for TQ under the thermal ionization mechanism. This model successfully predicted the experimentally observed TQ in 29 Ce^{3+}- and Eu^{2+}-activated phosphors with RMSE less than 10%. It should be noted that, although this model is focused on oxide phosphors, it can be extended to other chemistries by adjusting the fitted parameters.

For QDs, irreversible quenching is due to the thermally induced permanent structural defects that increase the trap states [as shown in Fig. 1(d)].[49] The structural defects are mainly because of the lattice mismatch between core and shell materials that generate interfacial strain and favor dislocation of atoms. As temperature rises, the thermal expansion difference of core and shell materials may result in the formation of permanent trapping centers. It should be noted that in the high-temperature synthesis process of QDs, although the temperature is much higher (typically 200–350 °C), the TQ did not occur since the QDs are in a high chemical potential environment with excessive ligands and precursors.[50] The reversible quenching mechanisms of QDs may not be explained by the traditional theories, i.e., the crossover theory [Fig. 1(b)] and multi-phonon relaxation theory [Fig. 1(c)]. Instead, Zhao *et al.* proposed that a thermally created temporary trap state or thermally activated trapping process may be the underlying mechanisms of the reversible quenching, as shown in Fig. 1(e).[49] After cooled down, the temporary traps relax back and the quantum yield (QY) is restored. In addition, the TQ mechanisms vary in different QD systems and further studies are necessary to obtain further understanding of the quenching mechanisms of QDs.

B. Heat dissipation in photoluminescent composites

Once the thermal phonons are generated from the photoluminescent particles, they shall be dissipated out to the ambient by overcoming a series of thermal resistances. Since the thermal resistance is strongly related to the packaging structure, the heat dissipation condition of photoluminescent composites varies a lot from package to package.[51–53] Figure 2 shows three typical packaging structures of WLEDs/WLDs with photoluminescent composites and their thermal resistance network. Generally, the on-chip type packaging is better than the remote type packaging for the heat dissipation of photoluminescent composites because the composites are directly contacted with highly thermal-conductive substrates. Moreover, all the thermal phonons must pass through the polymer matrix of photoluminescent composites before they can be dissipated out to the ambient air. Due to the extremely low thermal conductivity of polymer [<0.3 W/(m K)], the thermal resistance of polymer matrix is much larger than other components and dominates the total thermal resistance. For example, $R_{j\text{-}a}$ is in the range of 11.05–12.37 K/W according to our previously measurement results,[54] while $R_{ph\text{-}j}$ can easily reach 104 K/W [thermal conductivity $k = 0.17$ W/(m K), average thickness $\delta = 0.5$ mm, average radius $r = 3$ mm, $R_{ph\text{-}j} = \delta/(k \cdot \pi r^2)$]. Therefore, from the aspect of thermal resistance, reducing the thermal resistance of photoluminescent composites is critical for efficient heat dissipation toward photoluminescent particles. Moreover, the thermal interfacial resistance (TIR) of thermal interfacial materials (TIMs) in the package is also influential to the whole thermal dissipation process,[55,56] but it is beyond the scope of this paper. We focus on the heat manipulation of photoluminescent composites.

III. INSIDE THERMAL MANAGEMENT PROGRESS

As discussed above, the thermal resistance of photoluminescent composites is the dominant factor that affects the efficient heat dissipation of photoluminescent composites. In recent years, with the increase in input electronic power and the concentration of light beams (particularly in WLDs), the heat power generated in photoluminescent composites is thereby increased rapidly, which is detrimental to the optical efficiency and lifetime of photoluminescent particles. To solve this problem, peer researchers have devoted their effort to revealing and controlling the heat transport in photoluminescent composites. In this section, recent progresses in the modeling and manipulation of heat generation and dissipation of photoluminescent composites are summarized.

A. Modeling of heat generation and dissipation in photoluminescent composites

During the photoluminescence process, the photoluminescent particles absorb a certain number of short-wavelength photons and convert part of the absorbed photons into long-wavelength photons. The energy conversion efficiency η_{con} of a single photoluminescent particle can be expressed as follows:

$$\eta_{con} = \frac{N_{emitted}}{N_{absorbed}} \frac{hc}{hc} \frac{\lambda_{emitted}}{\lambda_{absorbed}} = \eta_{QE} \frac{\lambda_{absorbed}}{\lambda_{emitted}}, \quad (1)$$

where η_{QE} is the quantum efficiency of photoluminescent particles. Due to the nonradiative recombination processes, η_{QE} is usually below unit. For conventional Ce^{3+}-doped phosphors, η_{QE} is in the level of 0.8–0.9,[57,58] and the data are very close to 1 for QDs thanks to the innovation iterations in synthesis routes, such as by utilizing the intrinsic spin–orbit coupling of II–VI semiconductors,[59] by colloidal organometal halide perovskite QDs with an amorphous structure,[60] and by reducing the surface defect of perovskite QDs with surface passivation.[61]

Only obtaining η_{QE} is not enough to calculate the heat generation in photoluminescent composites because the total energy conversion efficiency of photoluminescent composites, which is defined as the ratio of output light energy to input light energy, is strongly related to the absorption, scattering, and anisotropy properties of photoluminescent composites. Therefore, the absorption coefficient (μ_a), scattering coefficient (μ_s), and anisotropy coefficient (g) are proposed to characterize the light propagation and conversion process in the photoluminescent composites, as shown in Fig. 3.

Together with η_{QE}, the heat generation can be calculated out accordingly. Since μ_a, μ_s, and g vary with particle species, size, concentration, and distribution, these parameters are hard to calculate theoretically. Therefore, Xie *et al.* proposed a precise optical

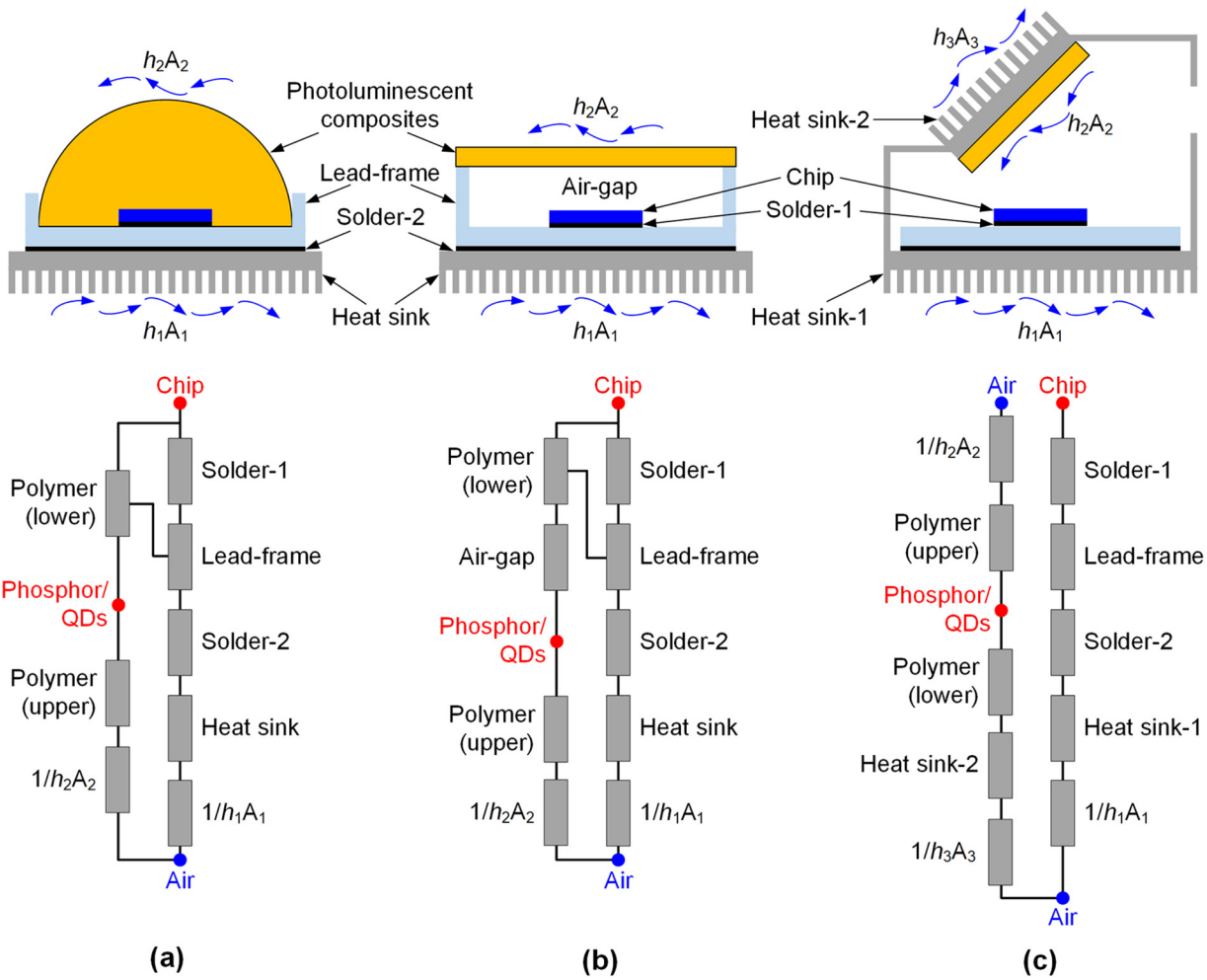

FIG. 2. Typical packaging structures of WLEDs/WLDs and their corresponding thermal resistance networks. (a) On-chip type. (b) Remote-transmissive type. (c) Remote-reflective type.

modeling method to calculate these parameters by combining double integrating sphere (DIS) measurement with the inverse adding-doubling (IAD) algorithm.[62] The transmittance, reflectance, and collimating transmittance of the photoluminescent composite samples were first measured by the DIS system. Then, the corresponding μ_a, μ_s, and g were calculated by the IAD algorithm. Subsequently, the heat generation in photoluminescent composites can be obtained by adopting these parameters into the Monte Carlo ray tracing simulation. Since the calculated data are based on the measurement results, the modeling accuracy is guaranteed with a maximum deviation of 1.16% (Fig. 4).

Considering the heat dissipation of photoluminescent composites in a WLED/WLD package, Lenef *et al.* combined the diffusion–approximation radiation transport model with the finite element method (FEM) to study the thermal effects of WLDs.[63,64] Hu *et al.* also have established a phosphor scattering model based on the Kubelka–Munk (K–M) theory to study the phosphor heating effects in WLEDs.[65,66] However, the above models assume that the QE of photoluminescent particles is constant, which is inappropriate because the QE is temperature-dependent.

To tackle this problem, Ma *et al.* proposed an opto-thermal model,[67] which combines the thermal resistance model with the K–M theory. According to the thermal resistance model, the working temperature of photoluminescent composites T_{ph} is derived as

$$T_{ph} = T_a + R_{total} \cdot Q_{ph}, \tag{2}$$

where T_a is ambient temperature and R_{total} is the total thermal resistance from the composites to the ambient. Q_{ph} is the heat generation of photoluminescent composites, which can be calculated by the K–M theory. In addition, the TQ effect is considered by iteratively calculating Q_{ph} and T_{ph} with a temperature-dependent QE. By using this

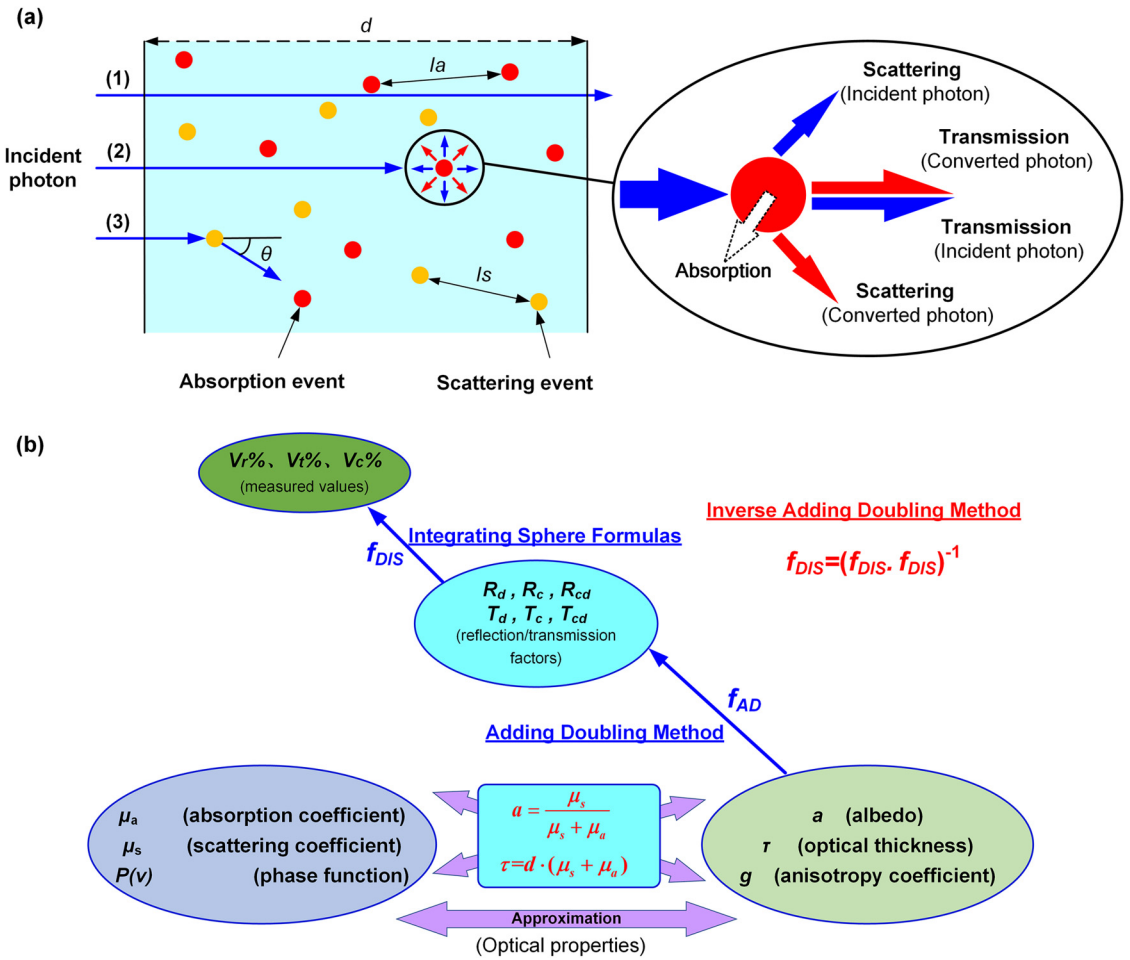

FIG. 3. Schematic showing all the possible behaviors between incident light and the photoluminescent composites. From Xie *et al.*, Sci. Rep. **7**, 16663 (2017). Copyright 2017 Author(s), licensed under a Creative Commons Attribution (CC BY) license.

model, we observed the sharp increase in phosphor temperature from 198 to 549 °C, which finally result in silicone carbonization.[67]

B. Manipulating heat dissipation in photoluminescent composites

In this section, we mainly review the strategies for efficient heat dissipation of photoluminescent composites, from the aspect of materials, processing, and packaging structures.

1. Phosphor-in-glass and single crystal phosphor

Typically, the photoluminescent composites are composed of photoluminescent particles (phosphors or QDs) and polymer matrix. Due to the intrinsically low thermal conductivity and thermally unstable property of polymer matrix, the conventional photoluminescent composites are incapable of dissipating the heat out quickly as well as maintaining the original optical performance of photoluminescent particles. To solve this problem, one of the effective strategies is to replace photoluminescent composites with phosphor-in-glass (PiG).[68–72] The PiG is fabricated by sintering the mixture of phosphor particles and glass powders under a relatively high temperature (600–1300 °C). Thanks to the glass component, the thermal conductivity of PiG [~0.6 W/(m K)] can be three times larger than that of traditional phosphor silicone [~0.18 W/(m K)]. Benefited from the reinforced thermal conductivity and thermal stability, the PiG demonstrates higher thermal stability than phosphor silicone. For example, when heated under 200 °C for 32 days, the PiG remains stable while the body color of silicone changes from colorless to browner.[69] Besides, Mou *et al.* demonstrated a reduction in the working temperature of 46 °C by substituting phosphor-in-silicone (PiS) with phosphor–sapphire–glass composites.[73] However, due to the necessity of a high-temperature sintering process, QDs cannot be prepared into such "QDs-in-glass"

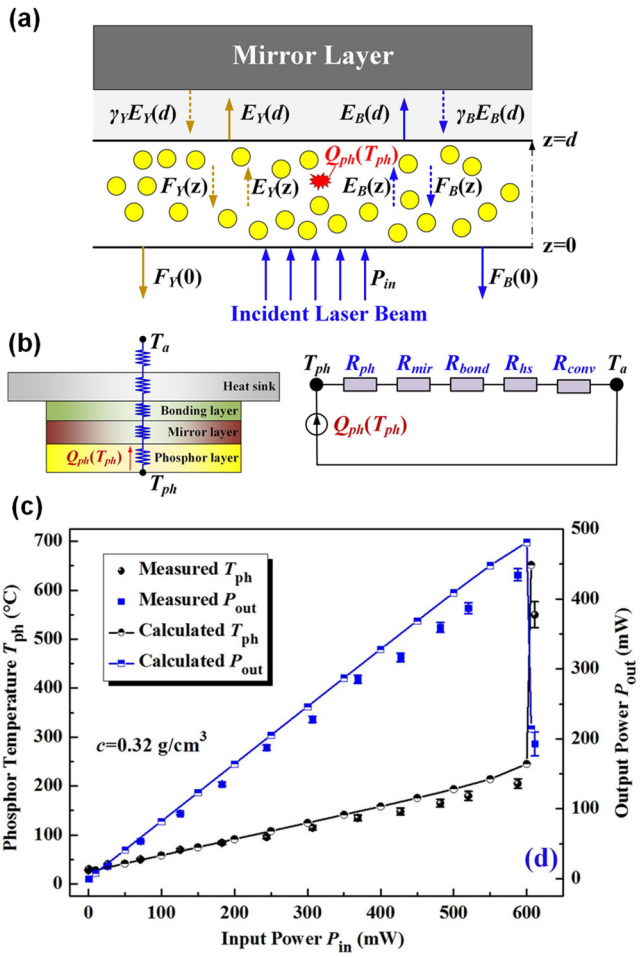

FIG. 4. Optical-thermal model consists of (a) a phosphor scattering model and (b) a thermal resistance model. (c) The calculated and measured phosphor temperature under a phosphor concentration of 0.32 g/cm^3. Reproduced with permission from Ma *et al.*, Int. J. Heat Mass Transfer **116**, 694 (2018). Copyright 2018 Elsevier.

composites because this high temperature may cause decomposition of QDs. Thus, the application of this method is limited.

Moreover, the single-crystal phosphor (SCP) was also proposed to significantly enhance the thermal conductivity of photoluminescent composites.[74,75] SCP is fabricated by the Czochralski (Cz) technique. Due to the less impurity and more rigid crystallization, the SCP exhibits an extremely high QE of 95% even under room temperature of 300 °C.[74] Moreover, SCP demonstrates a much higher thermal conductivity [~14 W/(m K)] than the above-mentioned PiG of phosphor silicone, which enables rapid heat dispersion within the material. As shown in Fig. 5, when illuminated by LDs with an optical power of 2 W, the surface temperatures of the free-standing SCP sample, SCP in the inorganic binder (PhosCera) sample, and phosphor in the PhosCera sample were 69.7, 134.4, and 457.1 °C, respectively. Despite these superior properties, SCP still needs to

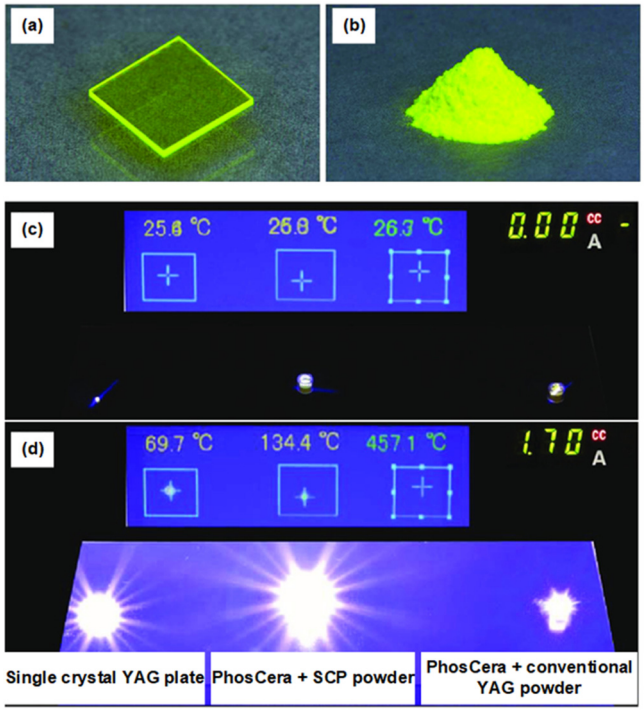

FIG. 5. (a) Single-crystal phosphor plate. (b) Single-crystal powder. Temperature rise of three different phosphors (SCP plate, PhosCera + SCP powder, PhosCera + CPP) with different LD intensities: (c) <10 mA and (d) 1.7 A. Reproduced with permission from Villora *et al.*, Proc. SPIE **9768**, 976805 (2016). Copyright 2016 SPIE.

solve the high cost and poor reproducibility problems before it can be widely utilized.

2. Polymer matrix reinforcement

A facile processing route is essential to prepare photoluminescent composites with reinforced thermal properties. Since the low thermal conductivity of photoluminescent composites is mainly due to the low thermal conductivity of polymer matrix, directly enhancing the thermal conductivity of polymer matrix seems a good idea. For bulk polymers, their crystallinity is relatively low due to the random arrangement of polymer chains and large molecule mass. The unordered crystal lattice and massive boundary defects lead to phonon scattering, resulting in low thermal conductivity.[76]

Therefore, enhancing the orientation and crystallization of polymer matrix is also a practicable strategy for enhancing the heat dissipation ability of photoluminescent composites. Zheng *et al.* fabricated a QD-polymer film by electrospinning.[77] During the electrospinning process, the polymer chains were stretched and redirected, and a composite film with higher orientation was obtained. Benefited from the aligned polymer chains in the electrospun nanofibers, the thermal conductivities in the through-plane and in-plane directions were enhanced by 39.9% and 423.1% at

25 °C, respectively. Consequently, the working temperature of QDs was decreased from 419 to 411 K at 200 mA. Actually, the thermal conductivity of the polymer matrix can be further enhanced by tuning the crystallization and orientation of polymer chains. For example, Lu *et al.* reported on polyethylene oxide (PEO) nanofibers with a maximum thermal conductivity of 28.84 W/(m K) by the electrospinning method, while the thermal conductivity of PEO bulk polymer is only 0.2 W/(m K).[78]

In addition to orienting the molecule chains by electrospinning, drawing or stretching can also orient the molecule chains of polymers. Shen *et al.* prepared a polyethylene (PE) fiber which consists of almost single crystals with a diameter of 50–500 nm after stretching, and the thermal conductivity is up to 104 W/(m K).[79] Such a high thermal conductivity is mainly due to the restructuring of the polymer chains by stretching that improves the fiber quality toward a "single crystalline fiber." This phenomenon can also be found in amorphous polymer fibers since Singh *et al.* reported that the thermal conductivity of polythiophene fibers in the amorphous state could reach 4.4 W/(m K).[80]

It should be noticed that these exciting progresses regarding the thermal reinforcement of polymer matrix are in the microscale or mesoscale. The macroscale and scalable fabrication of these highly ordered polymer matrices remains challenging yet attractive.

3. Thermally conductive fillers embedding

Compared to reinforcing the thermal conductivity of polymer matrix, incorporating highly thermal-conductive fillers into the photoluminescent composites is a more feasible strategy for enhancing their thermal conductivities. This is also the most widely used method in the research area of thermal interface materials (TIMs).[81,82] However, things get complicated when this method is utilized in photoluminescent composites, because most of the reinforcing fillers, such as metal-based fillers, ceramic fillers, and carbon-based fillers, are light-absorbing materials that will deteriorate the optical performance of photoluminescent composites.[83–85]

After persistent trials, we found that hexagonal boron nitride (hBN), known as "white graphene," is a suitable candidate for thermal reinforcing fillers for photoluminescent composites. We have validated that under a low filler loading of 4.3 wt. %, hBN successfully enhanced the heat dissipation of photoluminescent composites, and the maximum working temperature was reduced by 22.7 °C at 300 mA,[86] without sacrificing the luminous efficiency of WLEDs. The temperature reduction is mainly attributed to the highspeed heat dissipation pathway provided by hBN platelets. However, since hBN presents anisotropy thermal conductivity with a through-plane value of 20 W/(m K) and an in-plane value of 300–600 W/(m K),[87,88] the randomly distributed incorporating has not utilized the maximum thermal conducting ability of hBN platelets. To prepare photoluminescent composites with anisotropic distributed hBN platelets, whose in-plane directions are in the immediately thermal dissipation direction may be a better option. Therefore, we proposed an ice-templated method to fabricate the vertically thermal-conductive QD/hBN composites and WLEDs.[89] To avoid the unacceptable absorption toward light during the preparation, we substituted the graphene oxide by sodium carboxymethylcellulose (SCMC) as a cross-linking agent. With the crystallization of vertical ice templates in the freezing process, the hBN platelets alter their orientations under the action of torque and finally form the vertically arranged distribution. Based on these vertical enhanced QD/hBN composites, the maximum working temperature of WLEDs was 21 °C lower than the conventional WLEDs under the same driving current. Moreover, hBN can be combined with other materials to realize functions beyond heat dissipation. Xie *et al.* proposed a sandwich structural QD-SiO_2-BN nanoplate to enhance the heat dissipation as well as long-term stability of QDs in WLEDs.[90] QDs are first encapsulated by the SiO_2 shell to effectively defend water and oxygen penetration. Then, the QD-SiO_2 is embedded into the interlayer of layer-by-layer assembled BN nanoplates for fast heat dissipation. With these assembly structures, the working temperature of QDs is significantly reduced by 44.2 °C. After aging for 250 h, the photoluminescence (PL) intensity of QD-WLEDs only shows a slight degradation of 1.2%. The above strategies have validated the effectiveness of thermally conductive but optically nonabsorptive fillers in the heat dissipation enhancement of photoluminescent composites. Although nonabsorptive fillers are promising for the heat dissipation enhancement of luminescent composites, one drawback of this strategy is that the scattering effect inside the luminescent composites will also be enhanced with the increase in fillers loading. This will increase the reabsorption energy loss of luminescent particles, consequently increasing the heat generation of the composites. Therefore, countermeasures must be proposed to solve this problem. Recently, Li *et al.* proposed a solution to reduce the reabsorption loss of QD composites by incorporating QDs into SBA-15 particles.[91] Benefitted from the pore boundary structure of SBA-15, the incident light can be totally internal-reflected; thus, the reabsorption process is suppressed. As a result, WLEDs fabricated based on this technique achieved a high luminous efficacy that exceeds 200 lm/W. Therefore, it is believed that the simultaneous enhancement of heat dissipation and optical efficiency is achievable if multiple techniques are combined (Fig. 6).

4. Novel packaging structures

Since the working temperature of photoluminescent composites is strongly related to the heat generation and total thermal resistance of WLED/WLD packaging, changing and optimizing the packaging structure of WLEDs/WLDs is a direct strategy for realizing less heat generation and faster heat dissipation toward photoluminescent composites.

From the aspect of reducing heat generation, to separate photoluminescent particles with different emission wavelengths is a commonly used method. Yu *et al.* investigated the optical and thermal performance of three different WLEDs, including QD-phosphor mixed type, QD-inside type, and QD-outside type.[92] Their results show that the QD-outside type WLEDs show a 27% decrease of maximum nanocomposite temperature at 400 mA compared with the mixed-type WLEDs. This temperature reduction is attributed to the reduced reabsorption between phosphor and QDs; thus, the total heat generation is reduced. Similarly, we have validated that the vertically separated phosphor-QD layer structure is also beneficial for reducing their

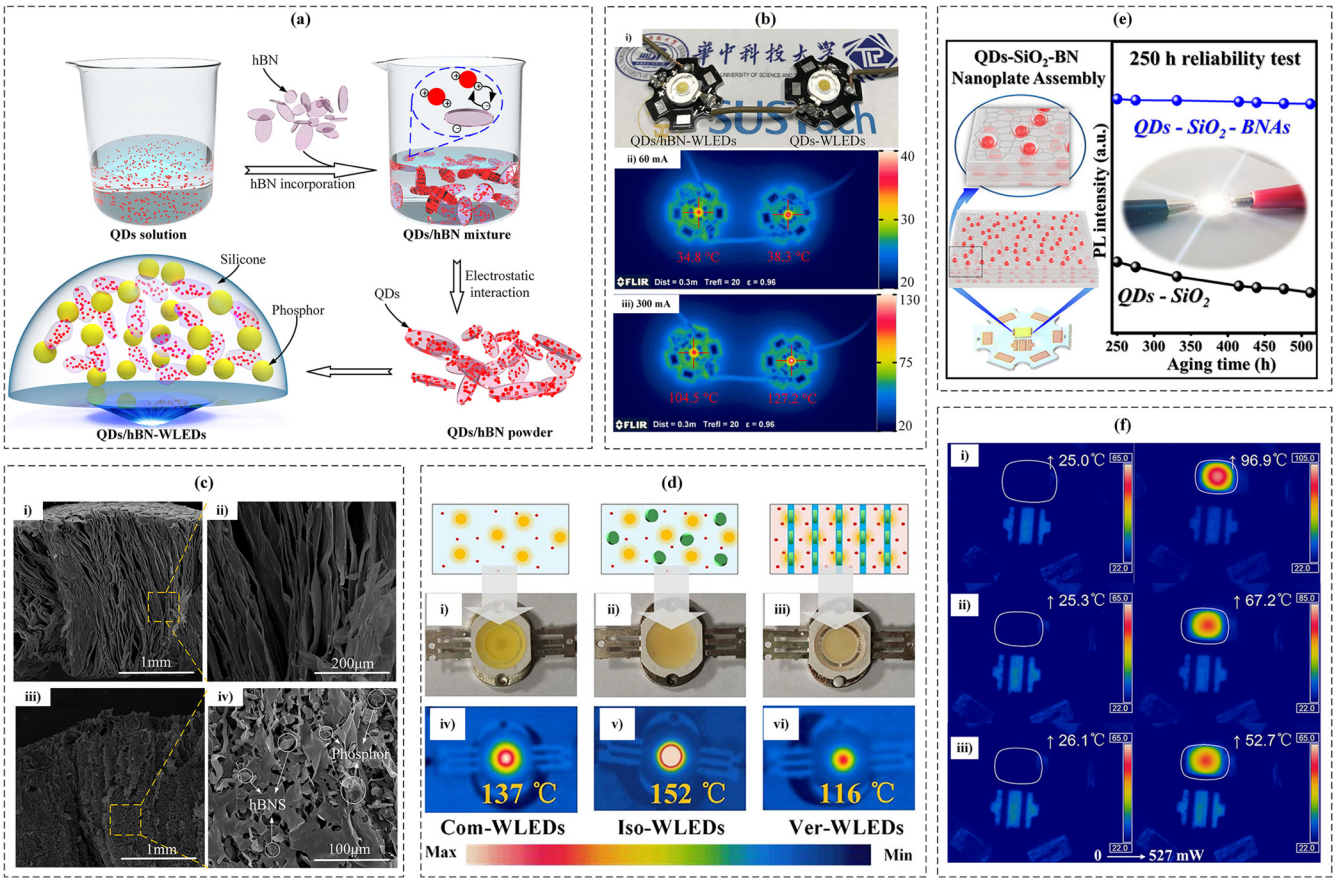

FIG. 6. (a) Schematic showing the preparation of QDs/hBN composites and the fabrication of QDs/hBN-WLEDs. (b) (i) Photograph of the QDs/hBN-WLEDs and QDs-WLEDs. (ii) and (iii) show the measured temperature fields of these two WLEDs at 60 and 300 mA, respectively. Reproduced with permission from Xie *et al.*, Adv. Funct. Mater. **28**, 1801407 (2018). Copyright 2018 John Wiley & Sons. (c) (i) and (ii) show the scanning electron microscope (SEM) images of the SCMC skeleton in a direction parallel to the surface of the templates. (iii) and (iv) show the hBN/SCMC/phosphor skeleton in a direction perpendicular to the template surface. (d) The measured templated fields of conventional QD-WLEDs [(i) and (iv)], isotropic-enhanced QD-WLEDs [(ii) and (v)], and vertical enhanced QD-WLEDs [(iii) and (vi)]. Reproduced with permission from Zhou *et al.*, ACS Appl. Nano Mater. **3**, 814 (2020). Copyright 2020 American Chemical Society. (e) Schematic showing the QD-SiO_2-boron nitride nanoplate assembly (BNAs) and their WLEDs. (f) The measured temperature fields of the WLEDs fabricated with (i) QDs-SiO_2, (ii) QDs/BN, and (iii) QD-SiO_2-BNAs. Reproduced with permission from Xie *et al.*, ACS Appl. Mater. Interfaces **12**, 1539 (2020). Copyright 2020 American Chemical Society.

reabsorption loss and thus reducing the maximum working temperature.[93] At 300 mA, the QDs' working temperature can reach 30.3 °C.

From the aspect of enhancing heat dissipation, one of the main ideas is to attach the photoluminescent composites onto a highly thermal-conductive substrate. This strategy requires that the substrate is optically transparent or the whole system is in reflective type. For example, we proposed to stack the QD films on a phosphor–sapphire composite (PSC) plate.[94] The PSC was fabricated by sintering phosphor glass onto a highly thermal-conductive sapphire substrate for fast heat dissipation. Compared with the traditional WLEDs, the QD-PSC-based WLEDs gained a reduction in working temperature of 65 °C at 1000 mA. Furthermore, we proposed a heat-conducting PiG with dual-sapphire plates for WLDs.[95] The PiG sapphires were fabricated by sintering the phosphor glass film between two sapphire plates. Benefited from the dual-sapphire configuration, the PiG sapphires present a low working temperature (<50 °C) under various laser powers, while the working temperature of referenced PiG can easily exceed 150 °C at 4.5 W power after 60 s.

In the meantime, Li *et al.* proposed a liquid cooling remote QD film structure to realize the 100 W level application of QD-WLEDs.[96] In their prototype, the QD film was removed from the LED chip and was assembled on a transparent glass chamber filled with flowing water for extremely fast heat dissipation. Cooled by the flowing water with high thermal capacity, the QDs' temperature in this water-cooling remote structure was stabilized at 71 °C at a driving power of 100 W, while those in traditional remote structure and on-chip structures were 265 and 453 °C, respectively. Similarly, Li proposed a sealed liquid cooling system in which the phosphor film was immersed (Fig. 7).[97]

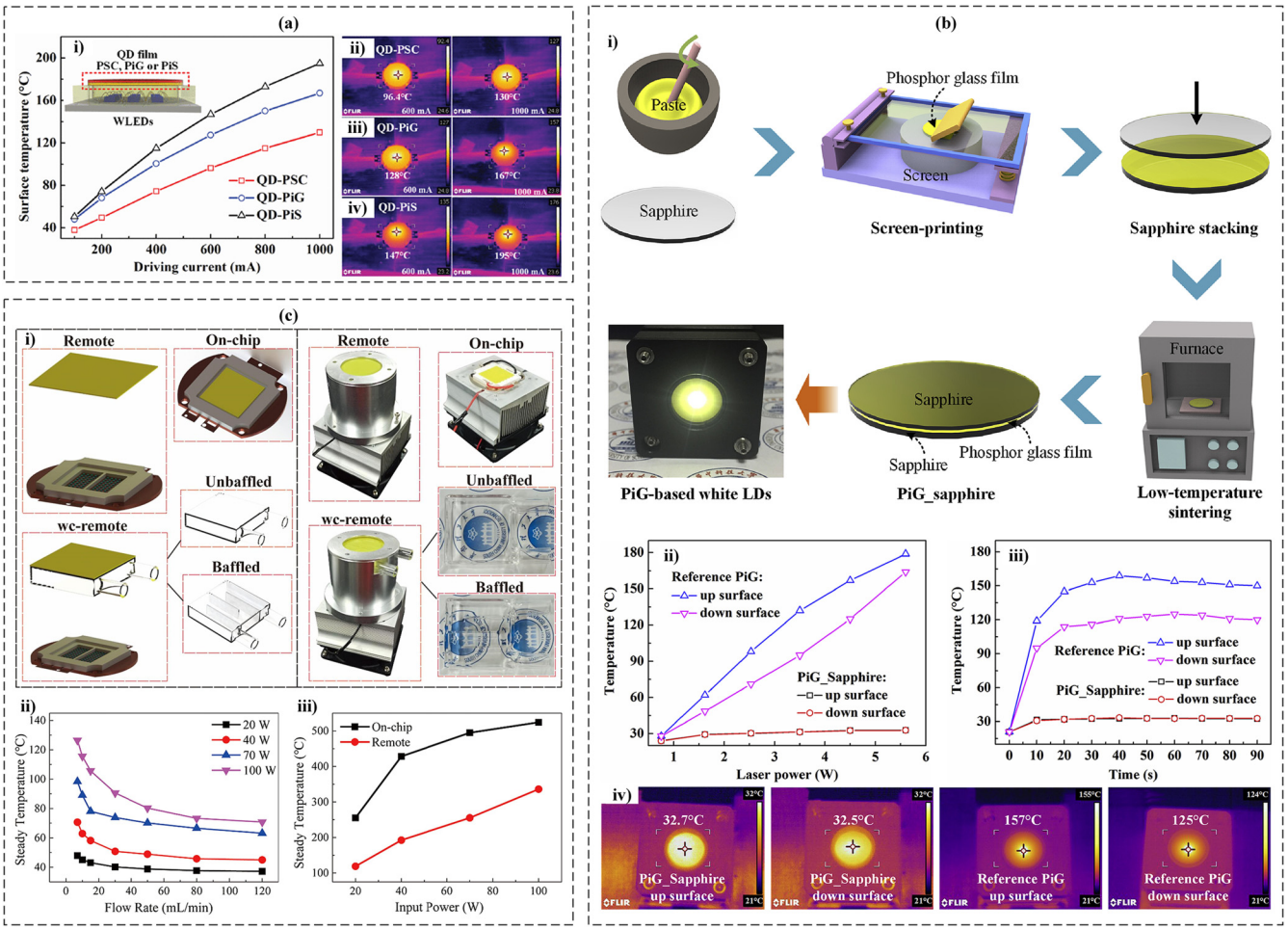

FIG. 7. (a) (i) Surface temperature of QD-PSC-, QD-PiG-, and QD-PiS-based WLEDs under different driving currents. Infrared thermal images of WLEDs packaged by (ii) QD-PSC, (iii) QD-PiG, and (iv) QD-PiS at 600 and 1000 mA, respectively. Reproduced with permission from Peng *et al.*, IEEE Trans. Electron Devices **66**, 2637 (2019). Copyright 2019 IEEE. (b) (i) Fabrication process of PiG_sapphire for WLDs. (ii) Working temperature of PiG_sapphire and reference PiG under different laser powers after the operation time of 60 s. (iii) Working temperatures of PiG_sapphire and reference PiG with the increase in operation time under a laser power of 4.5 W. (iv) Surface temperature images of PiG_sapphire and reference PiG at 4.5 W after 60 s. Reproduced with permission from Peng *et al.*, J. Alloys Compd. **790**, 744 (2019). Copyright 2019 Elsevier. (c) (i) Schematic diagram and photographs of the liquid cooling device structure for phosphor film. (ii) Maximum steady temperature of QD-WLEDs with the liquid cooling remote structure under different working conditions. (iii) Maximum steady temperatures of QD-WLEDs with traditional on-chip and remote structures under different input power. Reproduced with permission from Li *et al.*, Appl. Therm. Eng. **179**, 115666 (2020). Copyright 2020 Elsevier.

IV. SUMMARY AND OUTLOOK

In this Perspective, we have summarized the recent advances in heat manipulation theories and strategies of photoluminescent composites. Both the heat generation and transportation mechanisms and the recent progresses in heat manipulation of photoluminescent composites are discussed. We emphasize the package-inside thermal management solutions for WLEDs/WLDs since they are the most promising strategy for reducing the working temperature of photoluminescent composites, without deteriorating their optical performances. Despite great advances, there are still many challenges and opportunities in accelerating the maturation of this attractive field.

First, polymers such as silicone and epoxy are the main matrix for photoluminescent particles in WLEDs/WLDs, which are often thought to be thermally resistive materials due to their poor thermal conductivities [<0.5 W/(m K) in their amorphous state]. However, improved thermal conductivity of polymers by increasing their crystallite orientation and crystallinity has been constantly reported. The stretched film with a thermal conductivity of 65 W/(m K),[98] fibers with a thermal conductivity of 51 W/(m K),[99] and polyethylene nanofibers with a metal-like thermal conductivity of 104 W/(m K),[100] have shown huge potential in realizing highly thermal-conductive polymers in macroscopic scale. However, there is still a long way before the highly thermal-conductive bulk

polymers are produced. To achieve this goal, more intensive works should be carried out to uncover the thermal transport mechanisms of amorphous/aligned/crystalline polymers, and a novel manufacturing platform must be invented to realize micro-to-macro scale-up production toward highly thermal-conductive bulk polymers.

Second, before the breakthrough in thermal-conductive polymers was made, the most promising way for reinforcing the heat dissipation of photoluminescent composites is to construct an efficient thermal dissipation network inside the composites. As we have emphasized before, the established filler network must not deteriorate the photonic performance of WLEDs/WLDs. In this sense, both the filler type and filling volume fraction are limited. Currently, thermally conductive but optically nonabsorptive fillers are scarce. Ceramic fillers like boron nitride, aluminum oxide, and aluminum nitride can be adopted under a relatively low filling load but need a careful design on the filler network topology. Basically, under the same filling volume fraction, a three-dimensional (3D) interconnected network is superior to a single-directional aligned network in heat dissipation performance. However, the formation of a 3D network usually requires a large amount of fillers. Therefore, to construct a 3D thermal network in photoluminescent composites under a relatively low filling load is probably an optimal strategy for both optical and thermal design. However, state-of-the-art strategies for realizing a 3D thermal network, such as the magnetic-field assisted method,[101] the hot-pressing method,[102] and the templates-directed method,[103,104] are either high-temperature/pressure needed or extra light-absorbing additive needed, which cannot achieve the goal of high opto-thermal performance. To realize this goal, more works should be done to find a novel fabrication theory and methodology regarding the efficient construction of 3D heat dissipation network. Fortunately, peer researchers have already found some practical solutions, such as the air-bubbles-assembly method.[105,106]

Third, with the sharp rise of current density and heat flux density in light-emitting devices, the above-mentioned passive cooling strategies, including thermal-conductive polymers and 3D thermal network, toward photoluminescent composites may be insufficient in the foreseeable future. Therefore, active cooling designs with compact structures are expected to appear in the thermal management of photoluminescent composites. However, the-state-of-art active cooling solutions toward photoluminescent composites (mainly the liquid cooling) are far from compact, which is disadvantageous for practical applications for cooling photoluminescent composites.

ACKNOWLEDGMENTS

This work was supported by the National Natural Science Foundation of China (Nos. 51625601 and 52076087), the China Postdoctoral Science Foundation (No. 2021M691120), the Open Project Program of Wuhan National Laboratory for Optoelectronics (No. 2018WNLOKF017), the Creative Research Groups Funding of Hubei Province (No. 2018CFA001), and the Postdoctoral Creative Research Funding of Hubei Province.

DATA AVAILABILITY

Data sharing is not applicable to this article as no new data were created or analyzed in this study.

REFERENCES

[1]S. Tonzani, Nature **459**, 312 (2009).
[2]E. F. Schubert and J. K. Kim, Science **308**, 1274 (2005).
[3]S. Liu and X. Luo, *LED Packaging for Lighting Applications—Design, Manufacturing and Testing* (John Wiley & Sons, New York, 2016).
[4]X. Luo, R. Hu, S. Liu, and K. Wang, Prog. Energy Combust. Sci. **56**, 1 (2016).
[5]E. F. Schubert, J. K. Kim, H. Luo, and J. Xi, Rep. Prog. Phys. **69**, 3069 (2006).
[6]S. Nakamura and M. R. Krames, Proc. IEEE **101**, 2211 (2013).
[7]Y. Ma, L. Zhang, T. Zhou, B. Sun, Q. Yao, P. Gao, J. Huang, J. Kang, F. A. Selim, C. P. Wong, H. Chen, and Y. Wang, Chem. Eng. J. **398**, 125486 (2020).
[8]S. Nishiura, S. Tanabe, K. Fujioka, and Y. Fujimoto, Opt. Mater. **33**, 688 (2011).
[9]M. A. D. Maur, A. Pecchia, G. Penazzi, W. Rodrigues, and A. D. Carlo, Phys. Rev. Lett. **116**, 027401 (2016).
[10]M. Cantore, N. Pfaff, R. M. Farrell, J. S. Speck, S. Nakamura, and S. P. DenBaars, Opt. Express **24**, A215 (2016).
[11]S. Liang, M. Shang, H. Lian, K. Li, Y. Zhang, and J. Lin, J. Mater. Chem. C **5**, 2927 (2017).
[12]W. Chung, H. J. Yu, S. H. Park, B. H. Chun, and S. H. Kim, Mater. Chem. Phys. **126**, 162 (2011).
[13]J. J. Wierer, J. Y. Tsao, and D. S. Sizov, Laser Photonics Rev. **7**, 963 (2013).
[14]J. J. Wierer and J. Y. Tsao, Phys. Status Solidi A **212**, 980 (2015).
[15]P. C. Hung and J. Y. Tsao, J. Disp. Technol. **9**, 405 (2013).
[16]K. V. Chellappan, E. Erden, and H. Urey, Appl. Opt. **49**, F79 (2010).
[17]Nippon Electronic Company, see https://assets.sharpnecdisplays.us/documents/pressreleases/nc2402ml_pressrelease.pdf for NEC display solutions announces world's first digital cinema projector with replaceable laser module (2019).
[18]J. J. Wierer, J. Y. Tsao, and D. S. Sizov, Phys. Status Solidi C **11**, 674 (2014).
[19]L. Ulrich, *BMW Laser Headlights Slice Through the Dark* (BMW, Munich, 2013), see https://spectrum.ieee.org/transportation/advanced-cars/bmw-laser-headlights-slice-through-the-dark?tdsourcetag=s_pcqq_aiomsg (accessed 5 August 2019).
[20]J. Wanka, *Photonics in Germany* (BMW, Munich, 2017), see https://agustos.com/wp-content/uploads/2018/07/BMW-Article-Photonics-in-Germany-2017.pdf (accessed 5 August 2019).
[21]V. Heiskanen and M. R. Hamblin, Photochem. Photobiol. Sci. **17**, 1003 (2018).
[22]K. S. Cho, E. K. Lee, W. J. Joo, E. Jang, T. H. Kim, S. J. Lee, S. J. Kwon, J. Y. Han, B. K. Kim, B. L. Choi, and J. M. Kim, Nat. Photonics **3**, 341 (2009).
[23]E. Jang, S. Jun, H. Jang, J. Llim, B. Kim, and Y. Kim, Adv. Mater. **22**, 3076 (2010).
[24]X. Li, Y. Wu, S. Zhang, B. Cai, Y. Gu, J. Song, and H. Zeng, Adv. Funct. Mater. **26**, 2435 (2016).
[25]Q. Wali, F. J. Iftikhar, M. E. Khan, A. Ullah, Y. Iqbal, and R. Jose, Org. Electron. **78**, 105590 (2020).
[26]J. Liu, N. Li, J. Jia, J. Dong, Z. Qiu, S. Iqbal, and B. Cao, Sol. Energy **181**, 285 (2019).
[27]K. M. Sim, A. Swarnkar, A. Nag, and D. S. chung, Laser Photonics Rev. **12**, 1700209 (2018).
[28]D. Hao, J. Zou, and J. Huang, InfoMat **2**, 139 (2020).
[29]H. Zhu, Y. Fu, F. Meng, X. Wu, Z. Gong, Q. Ding, M. V. Gustafsson, M. T. Trinh, S. Jin, and X. Zhu, Nat. Mater. **14**, 636 (2015).
[30]X. Wang, S. Yan, W. Li, and K. Sun, Adv. Mater. **24**, 2742 (2012).
[31]A. Aboulaich, M. Michalska, R. Schneider, A. Potdevin, J. Deschamps, R. Deloncle, G. Chadeyron, and R. Mahiou, ACS Appl. Mater. Interfaces **6**, 252 (2014).
[32]B. Chen, Q. Zhou, J. Li, F. Zhang, R. Liu, H. Zhong, and B. Zou, Opt. Express **21**, 10105 (2013).
[33]B. Xie, J. Zhang, W. Chen, J. Hao, Y. Cheng, R. Hu, D. Wu, K. Wang, and X. Luo, Nanotechnology **28**, 425204 (2017).
[34]Z. Wei and J. Xing, J. Phys. Chem. Lett. **10**, 3035 (2019).
[35]V. Bachmann, C. Ronda, and A. Meijerink, Chem. Mater. **21**, 2077 (2009).

[36]X. Luo, X. Fu, F. Chen, and H. Zheng, Int. J. Heat Mass Transfer **58**, 276 (2013).
[37]R. Hu and X. Luo, J. Lightwave Technol. **30**, 3376 (2012).
[38]X. Luo and R. Hu, Int. J. Heat Mass Transfer **75**, 213 (2014).
[39]J. H. Jo, M. S. Kim, C. Y. Han, E. P. Jang, Y. R. Do, and H. Yang, Appl. Surf. Sci. **428**, 906 (2018).
[40]L. Turyanska, A. Patane, M. Henini, B. Hennequin, and N. R. Thomas, Appl. Phys. Lett. **90**, 101913 (2007).
[41]S. Poncé, Y. Jia, M. Giantomassi, M. Mikami, and X. Gonze, J. Phys. Chem. C **120**, 4040 (2016).
[42]K. A. Denault, J. Brgoch, S. D. Kloss, M. W. Gaultois, J. Siewenie, K. Page, and R. Seshadri, ACS Appl. Mater. Interfaces **7**, 7264 (2015).
[43]Y. Zhuo, A. M. Tehrani, A. O. Oliynyk, A. C. Duke, and J. Brgoch, Nat. Commun. **9**, 4377 (2018).
[44]P. Dorenbos, J. Phys.: Condens. Matter **17**, 8103 (2005).
[45]G. Blasse and B. C. Grabmaier, *Luminescent Materials* (Springer Verlag, Berlin, 2016).
[46]J. Ha, Z. Wang, E. Novitskaya, G. A. Hirata, O. A. Graeve, S. P. Ong, and J. McKittrick, J. Lumin. **179**, 297 (2016).
[47]A. C. Duke, E. Finley, M. Hermus, and J. Brgoch, Solid State Sci. **60**, 108 (2016).
[48]M. Amachraa, Z. Wang, C. Chen, S. Hariyani, H. Tang, J. Brgoch, and S. P. Ong, Chem. Mater. **32**, 6256 (2020).
[49]Y. Zhao, C. Riemersma, F. Pietra, R. Koole, C. de Mello Donegá, and A. Meijerink, ACS Nano **6**, 9058 (2012).
[50]C. D. Donegá, Chem. Soc. Rev. **40**, 1512 (2011).
[51]B. Xie, R. Hu, and X. Luo, J. Electron. Packag. **138**, 020803 (2016).
[52]D. H. Lee, J. Joo, and S. Lee, Opt. Express **23**, 18872 (2015).
[53]B. Xie, W. Chen, J. Hao, D. Wu, X. Yu, Y. Cheng, R. Hu, K. Wang, and X. Luo, Opt. Express **24**, A1560 (2016).
[54]Y. Ma, R. Hu, X. Yu, W. Shu, and X. Luo, Int. J. Heat Mass Transfer **106**, 1 (2017).
[55]L. Tan, J. Li, K. Wang, and S. Liu, IEEE Trans. Electron. Packag. Manuf. **32**, 233 (2009).
[56]K. Zhang, Y. Chai, M. M. F. Yuen, D. G. W. Xiao, and P. C. H. Chan, Nanotechnology **19**, 215706 (2008).
[57]Y. Zhuang, C. Li, C. Liu, Y. Fu, Q. Shi, Y. Liang, and L. Xia, Opt. Mater. **107**, 110118 (2020).
[58]L. Xia, Y. Yue, X. Yang, Y. Deng, C. Li, Y. Zhuang, R. Wang, W. You, and T. Liang, J. Eur. Ceram. Soc. **39**, 3848 (2019).
[59]B. S. Mashford, M. Stevenson, Z. Popovic, C. Hamilton, Z. Zhou, C. Breen, J. Steckel, V. Bulovic, M. Bawendi, S. Coe-Sullivan, and P. T. Kazlas, Nat. Photonics **7**, 407 (2013).
[60]J. Xing, F. Yan, Y. Zhao, S. Chen, H. Yu, Q. Zhang, R. Zeng, H. V. Demir, X. W. Sun, A. Huan, and Q. Xiong, ACS Nano **10**, 6623 (2016).
[61]Y. Sun, X. Yang, W. Jiao, J. Wu, and Z. Zhao, ACS Appl. Electron. Mater. **3**, 415 (2021).
[62]B. Xie, Y. Cheng, J. Hao, W. Shu, K. Wang, and X. Luo, Sci. Rep. **7**, 16663 (2017).
[63]A. Lenef, J. Kelso, Y. Zheng, and M. Tchoul, Proc. SPIE **8841**, 884107 (2013).
[64]A. Lenef, J. Kelso, M. Tchoul, O. Mehl, J. Sorg, and Y. Zheng, Proc. SPIE **9190**, 91900C (2014).
[65]R. Hu, H. Zheng, J. Hu, and X. Luo, J. Disp. Technol. **9**, 447 (2013).
[66]Q. Chen, Y. Ma, X. Yu, R. Hu, and X. Luo, IEEE T. Electron Dev. **64**, 463 (2017).
[67]Y. Ma, W. Lan, B. Xie, R. Hu, and X. Luo, Int. J. Heat Mass Transfer **116**, 694 (2018).
[68]J. K. Chang, W. C. Cheng, Y. P. Chang, Y. Y. Kuo, C. C. Tsai, Y. C. Huang, L. Y. Chen, and W. H. Cheng, Proc. SPIE **9571**, 957103 (2015).
[69]X. Zhang, J. Yu, J. Wang, B. Lei, Y. Liu, Y. Cho, R. Xie, H. Zhang, Y. Li, Z. Tian, Y. Li, and Q. Su, ACS Photonics **4**, 986 (2017).
[70]P. Zheng, S. Li, L. Wang, T. Zhou, S. You, T. Takeda, N. Hirosaki, and R. Xie, ACS Appl. Mater. Interfaces **10**, 14930 (2018).
[71]Y. Peng, Y. Mou, H. Wang, Y. Zhuo, H. Li, M. Chen, and X. Luo, J. Eur. Ceram. Soc. **38**, 5525 (2018).
[72]Y. P. Chang, J. K. Chang, W. C. Cheng, Y. Y. Kuo, C. N. Liu, L. Y. Chen, and W. H. Cheng, Opt. Mater. Express **7**, 1029 (2017).
[73]Y. Mou, H. Wang, D. Liang, J. Liu, Y. Peng, and M. Chen, J. Non-Cryst. Solids **515**, 98 (2019).
[74]E. G. Villora, S. Arjoca, D. Inomata, and K. Shimamura, Proc. SPIE **9768**, 976805 (2016).
[75]T. W. Kang, K. W. Park, J. H. Ryu, S. G. Lim, Y. M. Yu, and J. S. Kim, J. Lumin. **191**, 35 (2017).
[76]S. J. Kim, C. M. Hong, and K. S. Jang, Polymer **176**, 110 (2019).
[77]H. Zheng, X. Lei, T. Cheng, S. Liu, X. Zeng, and R. Sun, Nanotechnology **28**, 265204 (2017).
[78]C. Lu, S. W. Chiang, H. Du, J. Li, L. Gan, X. Zhang, X. Chu, Y. Yao, B. Li, and F. Kang, Polymer **115**, 52 (2017).
[79]S. Shen, A. Henry, J. Tong, R. Zheng, and G. Chen, Nat. Nanotechnol. **5**, 251 (2010).
[80]V. Singh, T. L. Bougher, A. Weathers, Y. Cai, K. Bi, M. T. Pettes, S. A. McMenamin, W. Lv, D. P. Resler, T. R. Gattuso, D. H. Altman, K. H. Sandhage, L. Shi, A. Henry, and B. A. Cola, Nat. Nanotechnol. **9**, 384 (2014).
[81]D. Suh, C. M. Moon, D. Kim, and S. Baik, Adv. Mater. **28**, 7220 (2016).
[82]C. Ji, Y. Wang, Q. Ye, L. Tan, D. Mao, W. Zhao, X. Zeng, C. Yan, R. Sun, D. J. Kang, J. Xu, and C. P. Wong, ACS Appl. Mater. Interfaces **12**, 24298 (2020).
[83]G. Lian, C. C. Tuan, L. Li, S. Jiao, Q. Wang, K. S. Moon, D. Cui, and C. P. Wong, Chem. Mater. **28**, 6096 (2016).
[84]M. Wang, H. Chen, W. Lin, Z. Li, Q. Li, M. Chen, F. Meng, Y. Xing, Y. Yao, C. P. Wong, and Q. Li, ACS Appl. Mater. Interfaces **6**, 539 (2014).
[85]V. Goyal and A. A. Balandin, Appl. Phys. Lett. **100**, 073113 (2012).
[86]B. Xie, H. Liu, R. Hu, C. Wang, J. Hao, K. Wang, and X. Luo, Adv. Funct. Mater. **28**, 1801407 (2018).
[87]K. Zhang, Y. Feng, F. Wang, Z. Yang, and J. Wang, J. Mater. Chem. C **5**, 11992 (2017).
[88]C. Yuan, J. Li, L. Lindsay, D. Cherns, J. W. Pomeroy, S. Liu, J. H. Edgar, and M. Kuball, Commun. Phys. **2**, 43 (2019).
[89]S. Zhou, Y. Ma, X. Zhang, W. Lan, X. Yu, B. Xie, K. Wang, and X. Luo, ACS Appl. Nano Mater. **3**, 814 (2020).
[90]Y. Xie, D. Yang, L. Zhang, Z. Zhang, C. Geng, C. Shen, J. G. Liu, S. Xu, and W. Bi, ACS Appl. Mater. Interfaces **12**, 1539 (2020).
[91]J. Li, Y. Tang, Z. Li, J. Li, X. Ding, B. Yu, S. Yu, J. Ou, and H.-C. Kuo, ACS Nano **15**, 550 (2021).
[92]S. Yu, Y. Tang, Z. Li, K. Chen, X. Ding, and B. Yu, Photonics Res. **6**, 90 (2018).
[93]B. Xie, H. Liu, X. W. Sun, X. Yu, R. Wu, K. Wang, and X. Luo, J. Electron. Packag. **141**, 031001 (2019).
[94]Y. Peng, Y. Mou, T. Wang, H. Wang, R. Liang, X. Wang, M. Chen, and X. Luo, IEEE Trans. Electron Devices **66**, 2637 (2019).
[95]Y. Peng, Y. Mou, Q. Sun, H. Cheng, M. Chen, and X. Luo, J. Alloys Compd. **790**, 744 (2019).
[96]Z. Li, Y. Chen, J. Li, S. Liang, and Y. Tang, Appl. Therm. Eng. **179**, 115666 (2020).
[97]K. Li, Proc. SPIE **9005**, 900507 (2017).
[98]S. Ronca, T. Igarashi, G. Forte, and S. Rastogi, Polymer **123**, 203 (2017).
[99]B. Zhu, J. Liu, T. Wang, M. Han, S. Valloppilly, S. Xu, and X. Wang, ACS Omega **2**, 3931 (2017).
[100]Y. Xu, D. Kraemer, B. Song, Z. Jiang, J. Zhou, J. Loomis, J. Wang, M. Li, H. Ghasemi, X. Huang, X. Li, and G. Chen, Nat. Commun. **10**, 1771 (2019).

[101]L. Wu, M. Ohtani, M. Takata, A. Saeki, S. Seki, Y. Ishida, and T. Aida, ACS Nano **8**, 4640 (2014).
[102]H. Qu, L. Yin, Y. Ye, X. Li, J. Liu, Y. Feng, C. Chang, X. Zhou, F. Tsai, and X. Xie, Chem. Eng. J. **389**, 123466 (2020).
[103]T. Tokuno, M. Nogi, J. Jiu, T. Sugahara, and K. Suganuma, Langmuir **28**, 9298 (2012).
[104]Z. Tian, Y. Zhao, S. Wang, G. Zhou, N. Zhao, and C.-P. Wong, J. Mater. Chem. A **8**, 1724 (2020).
[105]X. Zhang, T. Zhang, Z. Wang, Z. Ren, S. Yan, Y. Duan, and J. Zhang, ACS Appl. Mater. Interfaces **11**, 1303 (2019).
[106]H. Yang, Z. Li, B. Lu, J. Gao, X. Jin, G. Sun, G. Zhang, P. Zhang, and L. Qu, ACS Nano **12**, 11407 (2018).